HAL open science

Nonlinear free surface motions close to a vertical wall. Influence of a local varying bathymetry

Yves-Marie Scolan, Olivier Kimmoun, Hubert Branger, Fabien Remy

To cite this version:

Yves-Marie Scolan, Olivier Kimmoun, Hubert Branger, Fabien Remy. Nonlinear free surface motions close to a vertical wall. Influence of a local varying bathymetry. 22th Water waves and floatting bodies symposium, Apr 2007, Plitvice, Croatia. pp.1-4. hal-00193012

HAL Id: hal-00193012

https://hal.science/hal-00193012v1

Submitted on 24 Apr 2023

HAL is a multi-disciplinary open access archive for the deposit and dissemination of scientific research documents, whether they are published or not. The documents may come from teaching and research institutions in France or abroad, or from public or private research centers.

L'archive ouverte pluridisciplinaire **HAL**, est destinée au dépôt et à la diffusion de documents scientifiques de niveau recherche, publiés ou non, émanant des établissements d'enseignement et de recherche français ou étrangers, des laboratoires publics ou privés.

Distributed under a Creative Commons Attribution 4.0 International License

Nonlinear free surface motions close to a vertical wall.

Influence of a local varying bathymetry

Y.-M. Scolan*, **O. Kimmoun***, **H. Branger****, **F. Remy***,

* Ecole Centrale Marseille, 13451 Marseille cedex 20, France, scolan@egim-mrs.fr

** IRPHE, 13383 Marseille cedex 13, France,

1) Introduction

We are concerned with breaking waves at a vertical wall. Particularly we examine the influence of the local varying bathymetry just below the vertical wall as described on the following figure.

The modelling is not a big challenge since many numerical wave tanks nowadays can tackle this problem. It could be a solver of Euler's equations coupled with a interface tracking algorithm like a VOF technique or a Level-Set technique. It could be more classically a solver based on potential theory. In any case it is well known that such models may suffer from instabilities; these spurious instabilities are usually smoothed out at the price of a loss of mass or energy. Another drawback of these models is the important computational resources required to carry out time simulations.

It is not our intention here to carry out another survey on all the possible methods by listing their advantages or drawbacks. Tuck (1998) already carried out such a detailed survey. In particular he pointed out the efficiency and robustness of algorithms like the so-called desingularized Integral Equation initially introduced by Krasny (1986) and further developed by Cao *et al.* (1991).

We use here the same method of solution. The tank is basically rectangular. Tuck (1998) proposed a way to derive Green function adapted to this geometry. For a rectangle, this is straightforward since a simple conformal mapping exists. When the bathymetry is not horizontal, a more complicated conformal mapping must be derived. In the present abstract, we expose the main outlines of the used conformal mappings. Applications are done for various shapes of the bathymetry.

In effect there are many situations where we meet this kind of configurations: it could be either the mild slope along the jetty or the chamfrein in the tanks of LNG carriers with however a much higher slope. Comparisons with available experimental data show the efficiency of the elaborated algorithms.

1) Conformal mapping

A succession of conformal transformations is used to turn the original physical fluid domain into a half space. The sketch below sums up these transformations.

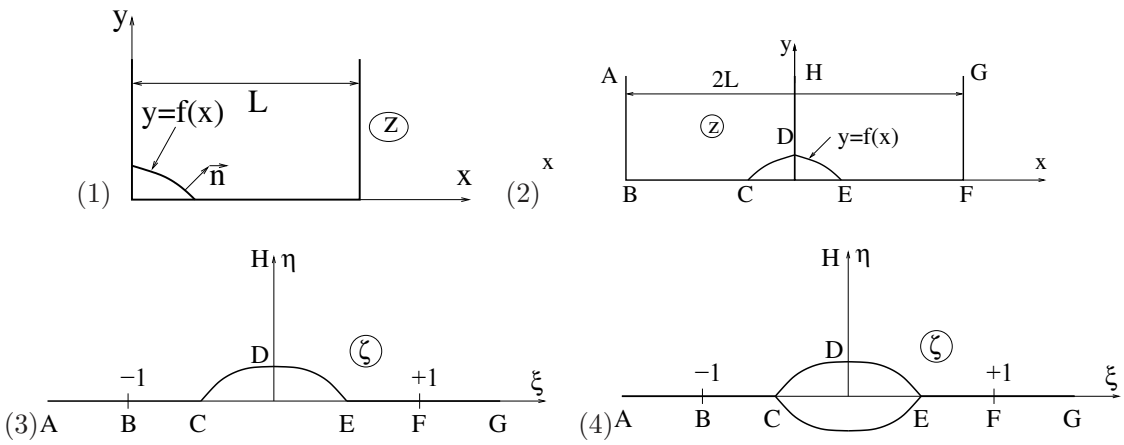

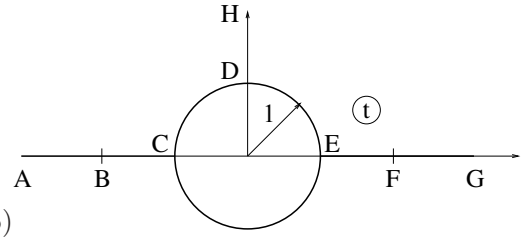

(5)

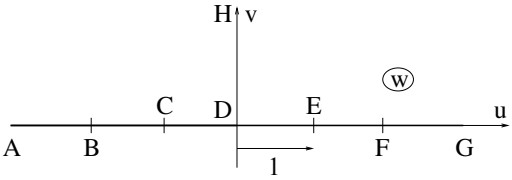

(6)

From the z-plane (plus its symmetric part with respect to the left vertical wall), we arrive at the ζ-plane by 'flattening' the two vertical walls. For that we use the transformation $\zeta = \sin \frac{\pi z}{2L}$. Then the symmetric domain with respect to the horizontal axis is introduced. The local bathymetry is now a closed contour which is transformed by using successively a Karman-Trefftz (KT) transformation and a Theodorsen-Garrick (TG) transformation; we arrive at a unit circle in the t-plane. Finally we use the transformation $w = \frac{1}{2}\left(t + \frac{1}{t}\right)$ to end up with the whole plane where the first quarter bounded by the positive real and imaginary axes corresponds to the image of the original fluid domain. It is not our intention to further develop these transformations. We shall rather focus on the Green function calculation.

2) Adapted Green function

We place a source at the origin of w-plane and we easily check that the boundary condition (impermeability) is satisfied on the solid walls, including the segment DH. The desingularized technique can be then implemented. The sources are introduced along a curve at a small distance from the actual position of the free surface. The velocity potential reads

$$\phi(x, y, t) = \sum_{j=1}^{N} q_j(t) G(x, y, X_j(t), Y_j(t)) \tag{1}$$

where (X_j, Y_j) are the source location and q_j is the strength of source j. For sake of simplicity the time dependency is now omitted. The Green function G is calculated in the w-plane as follows

$$G = \Re\left[F(w, \omega_j)\right] = \Re\left[\log(w - \omega_j) + \log(w + \omega_j) + \log(w - \overline{\omega_j}) + \log(w + \overline{\omega_j})\right] \tag{2}$$

where w and ω_j are the images of $z = x + iy$ and $Z_j = X_j + iY_j$ respectively, through the whole conformal mapping. The overline denotes the complex conjugate. The corresponding complex velocity is

$$\frac{dF_j}{dz} = \frac{dF_j}{dw}\frac{dw}{dz} = \frac{4w}{J}\left[\frac{w^2 - \Re(\omega_j^2)}{w^4 - 2w^2\Re(\omega_j^2) + |\omega_j^4|}\right] \tag{3}$$

where $J = \frac{dz}{dw}$ denotes the Jacobian of the transformation. Knowing that J is real on the real axis and on the segment DH, it is worth noticing that $\frac{dF}{dw}$ is real on the real axis and is purely imaginary on the segment DH. We can conclude that the normal velocity on the solid boundaries is identically zero there.

3) Nonlinear free surface equations

The time stepping is achieved by using a Runge-Kutta algorithm (fourth order) for the following time differential system

$$\frac{\mathrm{d}\Phi}{\mathrm{d}t} = \frac{1}{2}(U^2 + V^2) - g(y - h), \qquad \frac{\mathrm{d}X}{\mathrm{d}t} = U, \qquad \frac{\mathrm{d}Y}{\mathrm{d}t} = V \tag{4}$$

where (X, Y) are the cartesian coordinates of the lagrangian nodes at the free surface and (U, V) are the cartesian coordinates of the velocity. They are obtained from the spatial derivatives of the potential

$$U = \phi_{,x} = \sum_{j=1}^{N} q_j \Re\left[\frac{dF_j}{dz}\right], \quad \text{and} \quad V = \phi_{,y} = -\sum_{j=1}^{N} q_j \Im\left[\frac{dF_j}{dz}\right] \tag{5}$$

4) Applications

There is an easy way to simulate an overturning crest. That only depends on suitable initial conditions. Furthermore these initial conditions can be parametrized by a few parameters. Here we first defined the

initial free surface by $y = h + A\tanh(R(x - L/2))$ hence starting from rest with a given potential energy and a zero kinetic energy. Given the length L of the tank and the mean water depth h, varying the couple of parameters (A, R) allows to simulate a large range of wave shapes at the vertical wall. We can get an overturning crest at any given point of the tank or alternatively we can reproduce, by simply varying the mean depth, the overturning crest up to a focusing wave front, including the initiation of an entrapped air cavity. That is illustrated on the figures below

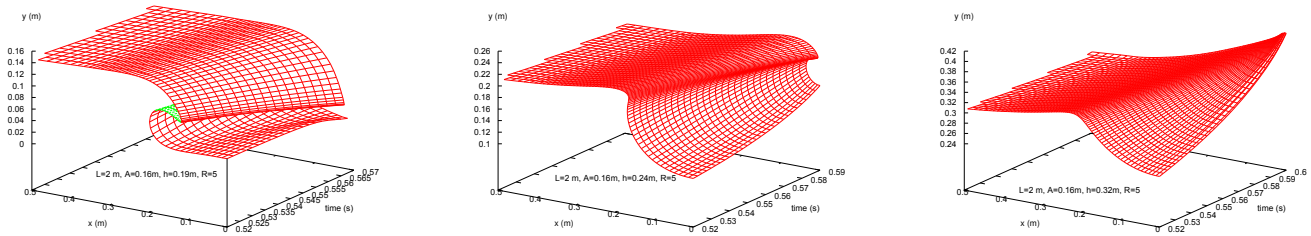

There is no hope to validate the present approach since the initial free surface deformation cannot be reproduced experimentally. However, thanks to the very fast algorithms (few seconds of CPU time on a standard PC for each run), we can cover a large space of parameters (A, R) and then identifications with available experimental data can be done. To this end, we use the results obtained within a PATOM project. These results consist of snapshots of the free surface and the corresponding velocity patterns obtained by a PIV device. These experiments were carried out in the wave flume of Ecole Centrale Marseille. This flume is described below

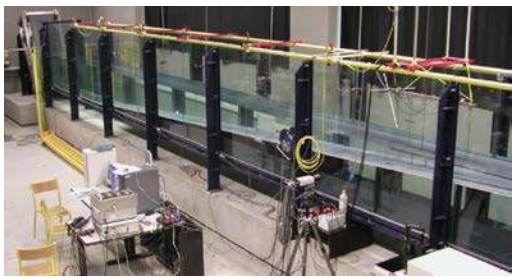

In these experiments a soliton is produced by a wavemaker. It propagates along a mild slope (1/15) up to breaking. Instead of the previous initial free surface, we used the following one $y = h + Ae^{-R(x-L)^2}$ For $L = 2m$ $A = 0.31m$, $h = 0.122m$ and $R = 4.3$, we can reproduce quite accurately the final instant $(t = 0.8635s)$ of the breaking as illustrated below

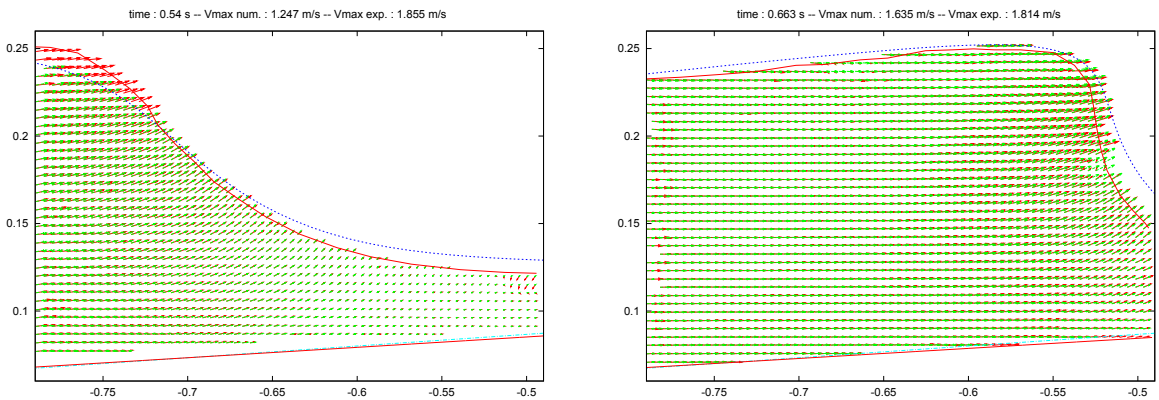

Then velocity patterns at three previous time instants are deduced. The velocity patterns are plotted above and below for $t = 0.54s$, $t = 0.663s$ and $t = 0.81s$. Due to the differences on the initial condition, the global errors on the identification increases as we come back in time. However the velocity patterns (both experimental and numerical ones) fits surprisingly well at any stage. It should be underlined the small

discrepancies on the maximum of the velocity. This data is crucial since it sets the intensity of the velocity throughout the studied pattern.

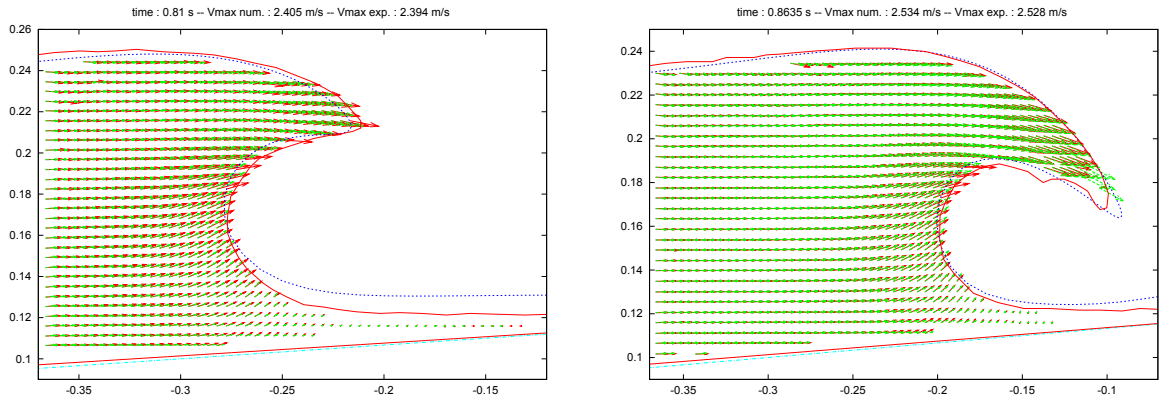

There are different way to quantify a relative error; it is calculated relatively to either the highest velocity or the local velocity. In the latter case obviously the relative error may be large, but in the former case the error is very small (less that 0.2 %). The area where the discrepancy is the highest, is mainly along the contour of the velocity pattern. The figures below zoom on the crest where the local error is calculated for the intensity of the velocity and its direction

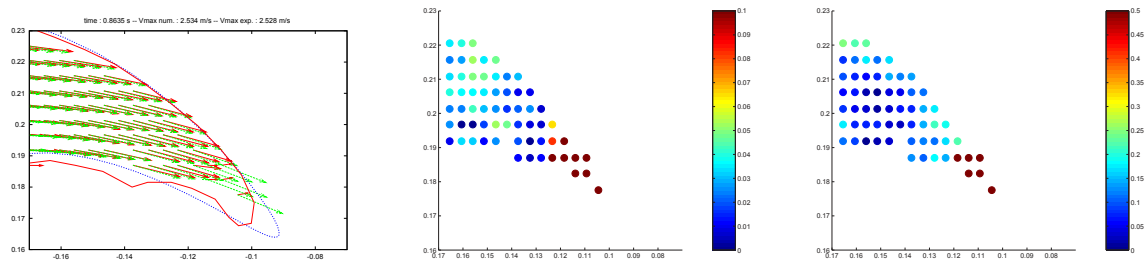

The PIV measurements in the tip of the crest seem difficult, but the relative error, especially for the intensity is quite reasonable that is to say in the range of the experimental error (about 5 %). It should be noted that these results cannot be considered as a strict validation of the model, but it proves that the local kinematics of an actual overturning crest can be easily simulated.

Other shapes of bathymetry are studied like elliptic or rectangular step. This will be shown during the workshop.

5) Conclusion

Following the tracks of Tuck (1998), it is shown that fast algorithms can be elaborated to simulate breaking waves. Here improvments have been brought to tackle varying bathymetry. To this end, conformal mappings are used to derive an adapted Green function. The robustness of the whole algorithms follows from the use of the desingularized Integral Equation developed by Cao *et al.* (1991).

Many types of bathymetry can be investigated. Here we focused on a mild slope for which experimental data are available. An identification procedure is performed since we solve the nonlinear free surface equations starting from a given potential energy, and not by modelling a real wave tank equipped with a wavemaker. The comparisons offer good confidence into the present approach. It also demonstrates that the model is reliable enough to predict the initial data to study the impact of the wave on the vertical wall. This is the next step of the present study.

6) References

• Krasny R., 1986, Desingularization of periodic vortex sheet roll-up, Journal of Computational Physics Vol. 65, Issue 2, 292–313

• Cao Y., W.W. Schultz & R.F. Beck, 1991, A three-dimensional desingularized boundary integral method for potential problems, Intl. J. Numer. Meth. Fluids 11 785-803.

• Tuck E.O., 1998, Solution of Nonlinear Free-Surface Problems by Boundary and Desingularised Integral Equation Techniques, CTAC'97, Singapore, 11-26.